PHYSICAL REVIEW MATERIALS **1**, 051402(R) (2017)

Ferroelectric domain wall phonon polarizer

Miquel Royo,[1,*] Carlos Escorihuela-Sayalero,[2] Jorge Íñiguez,[2,†] and Riccardo Rurali[1,‡]
[1]*Institut de Ciència de Materials de Barcelona (ICMAB–CSIC) Campus de Bellaterra, E-08193 Bellaterra, Barcelona, Spain*
[2]*Materials Research and Technology Department, Luxembourg Institute of Science and Technology, 41 rue du Brill, L-4422 Belvaux, Luxembourg*
(Received 11 April 2017; published 31 October 2017)

Modulating the polarization of a beam of quantum particles is a powerful method to tailor the macroscopic properties of the ensuing energy flux as it directly influences the way in which its quantum constituents interact with other particles, waves, or continuum media. To date, practical polarizers, being well developed for electric and electromagnetic energy, have not yet been proposed for heat fluxes carried by phonons. Here, we report on atomistic phonon transport calculations demonstrating that ferroelectric domain walls can operate as phonon polarizers when a heat flux pierces them. Our simulations for the representative ferroelectric perovskite $PbTiO_3$ show that the structural inhomogeneity associated with the domain walls strongly suppresses transverse phonons, while longitudinally polarized modes can travel through multiple walls in series, largely ignoring their presence.

DOI: 10.1103/PhysRevMaterials.1.051402

Controlling heat conduction has always been a challenging task, to the point that our ability to manipulate thermal fluxes lags far behind our long-standing know-how in manipulating electric and electromagnetic fluxes. In solids, the principal complication in manipulating heat stems from the *a priori* impossibility to use electrical signals or electromagnetic fields for that purpose. This is because phonons, the dominant heat carriers in insulating materials, do not possess a bare charge.

Heat conduction can be instead, modulated following basically two fundamentally different approaches. In the first approach, the most extended one, structural inhomogeneities such as atomic-scale defects, materials interfaces, or surfaces, are incorporated in a physical material to scatter phonons diffusively and reduce the thermal conductivity [1,2]. In addition to this approach, which exploits the corpuscular nature of phonons, wave-interference phenomena have been recently demonstrated to effectively block the propagation of phonons traveling through periodic superlattices or phononic crystals [3–5]. Interestingly, both approaches offer the possibility to focus on a fixed frequency window, i.e., to perform a frequency filtering effect, by choosing the size of the structural inhomogeneities or their periodicity.

However, candidate systems to effectively filter phonons of a certain polarization, the so-called phonon polarizers, are yet to come forth. The only previous hints of a mode-dependent phonon scattering have been observed by means of ballistic phonon imaging techniques at very low temperatures (<3 K) in highly dislocated LiF crystals [6] and in an exotic ferroelectric such as KH_2PO_4 [7]. Nevertheless, in these systems a clear polarizer effect capable to discern between, at least, longitudinal and transverse phonons, was not observed. It has also been suggested that material interfaces enclosing a molecular self-assembled monolayer should exhibit a phonon-polarizing effect due to the anisotropy in the bond strength across the length and breadth of the monolayer [8], but such a conjecture has not yet been experimentally nor numerically proved. The polarization of phonons influences important physical phenomena wherein phonons participate. For example, the way in which phonons couple to defects and to electronic states depends markedly on their polarization, as well as on other defining properties such as their frequency and propagation direction. Likewise, phonons play an important role in nonradiative energy relaxation and interband recombination processes, which are known to be ruled by polarization-dependent selection rules. Therefore, the possibility to modulate the polarization of a flux of phonons at will would offer definite possibilities for modifying the behavior of materials and/or carrying information.

Here, we demonstrate that the ferroelectric interfaces occurring between polarization domains in a well-known perovskite oxide, $PbTiO_3$, can effectively operate as phonon polarizers. Such interfaces, also known as domain walls (DWs), are today routinely created, moved, and annihilated by the application of local electric fields [9–11], a possibility that renders them potential candidates to dynamically manipulate phonons with electrical signals and to enable *in situ* reconfigurable thermal circuiting within a given material volume. In fact, DW thermal transport engineering was already attempted in the last decades in ferroelastics [12,13] and ferroelectrics such as $BaTiO_3$ [14] and KH_2PO_4 [7,15], obtaining a remarkable modulation of the conductivity by means of strain and electrical alteration of the DW density in the crystals. Today, the focus is on ferroelectric thin films that permit a precise control of the spacing between DWs which, in turn, makes it possible to control the dominant scattering mechanism: For DW separations comparable to or below the average phonon mean free path, the phonon transport is dominated by the walls scattering rather than by anharmonic phonon-phonon interactions. Ihlefeld *et al.* [16,17] have recently proceeded in this way to prepare the first prototypes of electrically actuated DW thermal switches operating over a broad temperature range, including room temperature.

Little is known about the phonon spectral distribution in multidomain ferroelectrics. In particular, the mechanisms of phonon scattering at DWs have not yet been elucidated for any material to the best of our knowledge. Such a type of information is difficult to extract from experiments and typically requires the combined use of theory and numerical

*mroyo@icmab.es
†jorge.iniguez@list.lu
‡rrurali@icmab.es

simulations. In this regard, a theoretical study by Wang *et al.* [18] has dealt with the problem of simulating phonon transport through multidomain ferroelectrics. However, a continuum-level phase-field approach was used in which the DW phonon scattering mechanism is a required input, rather than an output, of the calculation. On the other hand, we have very recently demonstrated the harmonic character of the phonon scattering mechanism at prototypical $PbTiO_3$ DWs by contrasting nonequilibrium molecular dynamics and harmonic nonequilibrium Green's functions calculations [19].

Here, we report mode-resolved phonon transport calculations in multidomain ferroelectrics with an atomistic detail. To this end, we interface force-constant matrices obtained from second-principles model potentials (SPMP) [20] with mode-dependent nonequilibrium Green's function (NEGF) [21] methodologies. SPMP is a powerful approach, recently developed by one of us, to study ferroelectric lattice-related properties with the potential to provide a detailed atomistic picture of a temperature-driven DW formation [22], as well as to predict exotic properties such as negative capacitance in multidomain ferroelectric superlattices [23]. On the other hand, mode-dependent NEGF is an extension of the conventional NEGF method [24] to obtain the individual contribution of each phonon mode to the thermal transport. A thorough formulation of this method has been recently introduced in Ref. [21] and a specific description can be found in Ref. [25]. As a brief overview, the physical system is partitioned along the heat transport direction into a scattering region (channel) and two semi-infinite reservoirs (contacts), that are held at constant temperatures, and the problem consists in calculating the ballistic transmission probability of each phonon from one contact to the other across the channel. In the calculation we take advantage of the system periodicity in the plane perpendicular to the heat transport: By Fourier-transforming we can decouple a three-dimensional (3D) transport calculation into a set of one-dimensional (1D) calculations with different two-dimensional (2D) transverse wave vectors $\mathbf{k}_\perp$. The total measurable 3D magnitudes are then retrieved by integration over the 2D Brillouin zone.

An example of the atomistic computational supercell employed in the simulations is shown in Fig. 1. It consists of a tetragonal $PbTiO_3$ (PTO) lattice with the ferroelectric polarization oriented parallel to the z axis. In the case of the figure, two flat 180° DWs have been introduced in the channel. The DWs lie in the y,z plane, and are thus perpendicular to the transport direction x. As shown in Fig. 1(c), across the leftmost DW, the ferroelectric polarization P_z transits monotonically from positive to negative values, and vice versa across the rightmost DW. In addition, a spontaneous polarization along the y direction (P_y) is formed at the DWs and rapidly vanishes into the domains. According to Ref. [22], this polarization is switchable, so that parallel and antiparallel metastable configurations can in principle be induced in samples with more than one DW.

We begin the heat transport study by analyzing the total phonon transmission function and thermal conductance calculated for PTO samples with up to three DWs in a series in the channel. The results are shown in Fig. 2 together with those for a reference monodomain (0DW) sample. It is observed that the presence of a single DW reduces considerably the phonon

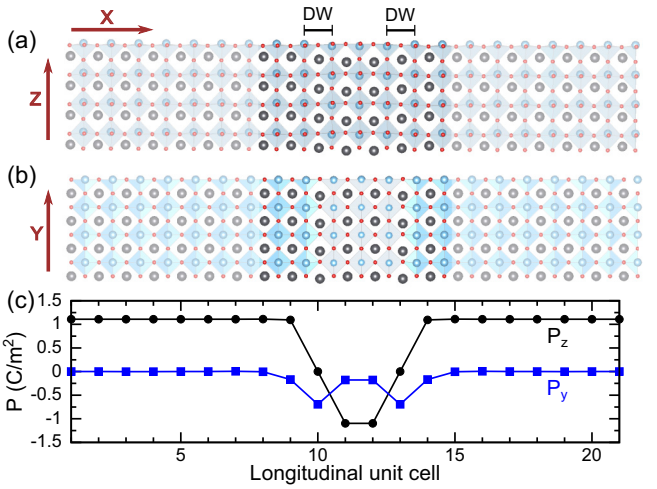

FIG. 1. Views of the (a) x,z and (b) x,y cross sections of a prototypical tetragonal PTO supercell employed in the computational simulations. Gray, blue, and red colors are used for Pb, Ti, and O atoms, respectively, and partial transparency is used to illustrate atomic positions in the homogeneous contacts. The channel includes two flat domain walls extending over a Pb-O (y,z) plane and separated by approximately two primitive cells. (c) shows the polarization profiles along the thermal transport direction x (the calculation of these local polarizations is described in Ref. [20]). Black and blue points show the calculated polarization components along z and y, respectively, while lines are a guide to the eye. A spontaneous P_y polarization arises at the DWs in addition to the monotonic inversion of P_z.

transmission. In particular, an efficient scattering is observed for phonons of a frequency higher than 35 THz. Interestingly, the DW does not work well as a low-pass phonon filter since a strong scattering is also observed for three low-frequency peaks. The lattice thermal conductance is strongly depleted by a single DW with a maximal reduction of ∼43% attained at $T \sim 25$ K and essentially related to the scattering of the low-frequency phonons. This is a remarkable effect, taking into account the coherent nature of the ideal DW we simulate.

The inclusion of a second DW in the channel further reduces the transmission and conductance, but its effect is much smaller than that of the first DW, a trend that is repeated for a third DW. Indeed, it seems that both transport magnitudes would tend towards an asymptotic limit if an increasing number of DWs in a series were included in the channel. This indicates that the DWs do not act on the thermal flux as series resistors; instead, most of the scattering is brought about by the first few DWs and some phonons travel across the multiple interfaces without being scattered. Similar asymptotic behaviors have been observed in other types of multicomponent layered systems with a few clean heterojunctions [26–28] and in superlattices [3]. We have also checked that the DW spacing has a negligible effect on the transport properties in the current ballistic regime (see Ref. [25]), although this is known to be a crucial factor when anharmonic umklapp processes become the dominant scattering mechanism at higher temperatures [16,17].

To elucidate the question of which phonons are being most effectively scattered by the DWs, we show in Fig. 3

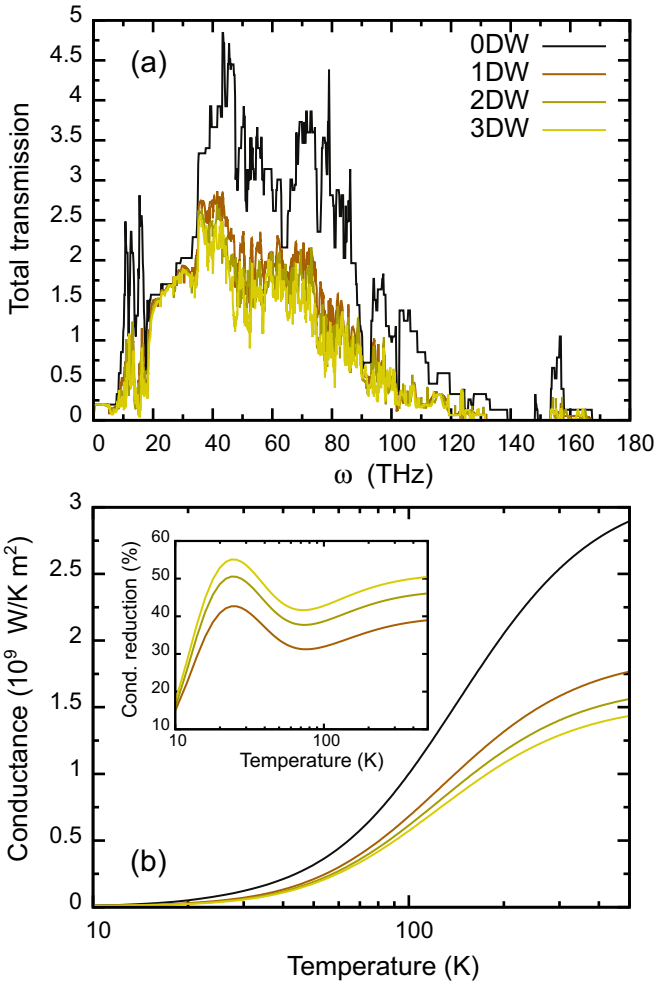

FIG. 2. (a) Total phonon transmission function and (b) thermal conductance calculated for PTO samples with zero, one, two, and three flat DWs in the channel. The inset in (b) shows the percent of conductance reduction with respect to the monodomain (0DW) system.

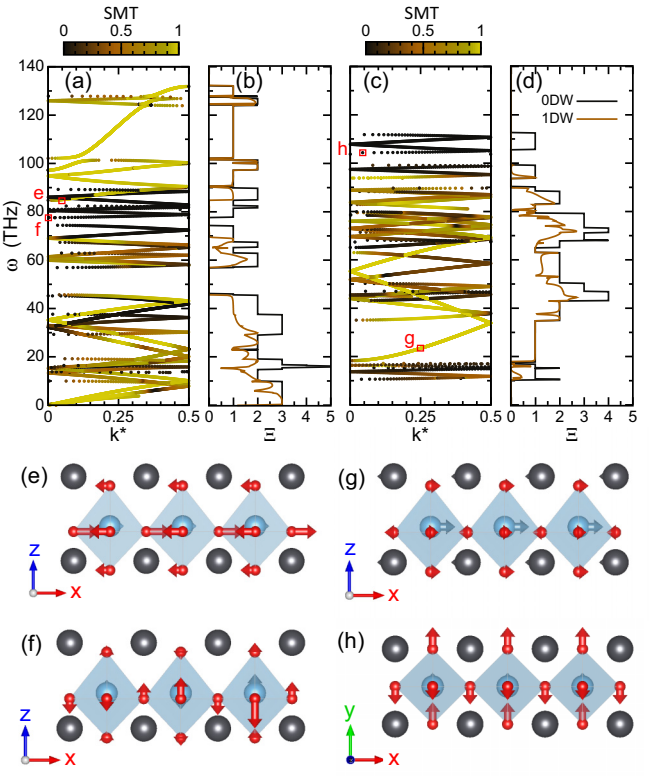

FIG. 3. Single-mode transmission analysis through a single DW shown for two selected values of $\mathbf{k}_\perp$. The dispersion of the left contact phonons (the right contact bands are equivalent) along the longitudinal reduced wave vector is shown in (a) and (c) for the transverse Brillouin zone center ($k_y^* = k_z^* = 0$) and zone edge ($k_y^* = k_z^* = 0.5$), respectively. The bands are four times folded because four primitive unit cells have been used to define the contact principal layer along the longitudinal direction. The color map illustrates the individual probability of transmission of each phonon mode. The transmission functions at a discrete transverse wave vector [$\Xi(\mathbf{k}_\perp,\omega)$] are obtained by summing over all phonon modes of (a) and (c) at a given frequency and are respectively shown in (b) and (d) and compared with the transmission function of a monodomain sample. Notice the integer values for the 0DW case that give the number of available phonon modes at a given ($\mathbf{k}_\perp,\omega$) point. (e)–(h) show with arrows the atomic displacements of the Γ-phonon modes with the highest contribution in the phonons indicated with red squares in (a) and (c). Gray, blue, and red colors are used for Pb, Ti, and O atoms, respectively.

the results of the single-mode transmission calculation at two discrete $\mathbf{k}_\perp$ points, namely, at the transverse Brillouin zone center [Figs. 3(a) and 3(b)] and zone edge [Figs. 3(c) and 3(d)]. The color map in Figs. 3(a) and 3(c) illustrates the probability of transmission of each individual phonon across a single DW and indicates that, as anticipated, some modes are completely scattered (black dots) while others are completely transmitted (light-yellow dots). One can even appreciate whole phonon bands with a well-defined character, scattered or transmitted, occurring at different frequency ranges. We can get more insight into the nature of the scattered and transmitted modes by analyzing their eigendisplacements. To this end, we project the lattice-periodic part of the eigenvectors of selected phonons, which in general have complex components, on the basis set formed from the phonon eigenvectors at the Γ point, which can be chosen to be real. We observe that the phonons scattered by the DW can be associated with the Γ modes whose corresponding atomic displacements are along the directions transverse to the heat flux, both parallel to the ferroelectric polarization [see Fig. 3(f)] as well as perpendicular to it [see Fig. 3(h)]. In contrast, transmitted phonon modes are associated with atomic displacements along the longitudinal direction [see Figs. 3(e) and 3(g)].

Phonons cannot be classified as purely transverse or purely longitudinal vibrational modes except at special points of the Brillouin zone. Here, we adopt a practical approach and identify as longitudinal modes those phonons whose eigenvectors present at least 70% polarization along the longitudinal x direction. We then quantify the observed polarization-filter effect by computing the phonon transmission function ($\mathcal{T}^L$) and thermal conductance (G^L) due to the transport of longitudinal phonons. In Figs. 4(a) and 4(b) we show $\mathcal{T}^L$ and G^L scaled by the total transmission function and thermal conductance, respectively, in order to obtain comparable results for systems

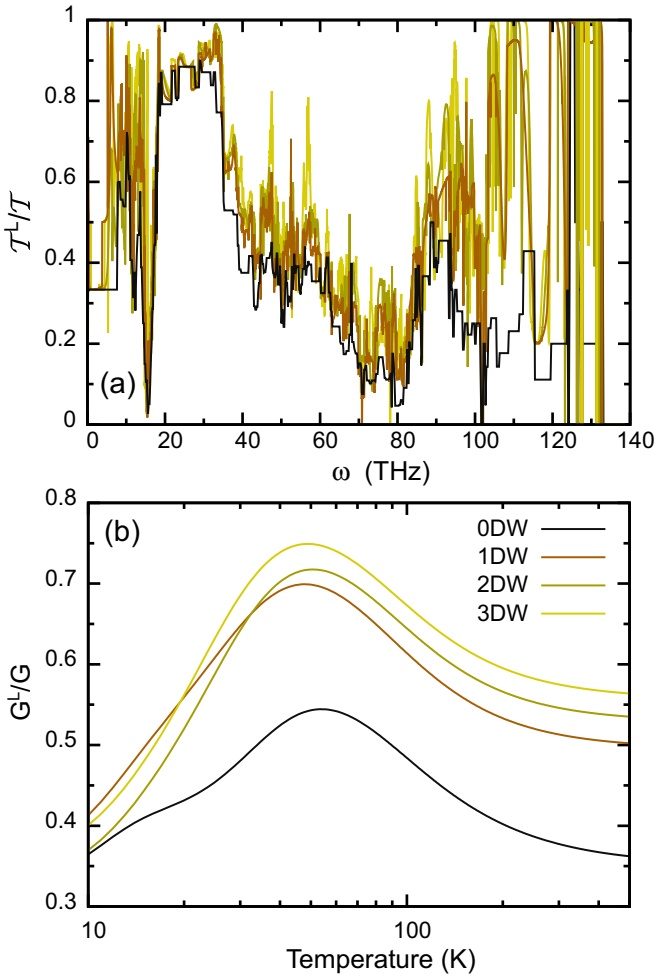

FIG. 4. Fraction of total phonon transmission function (a) and thermal conductance (b) due to phonons that are at least 70% polarized in the longitudinal direction for samples with a different number of DWs in series.

with a different number of DWs. In other words, we represent the fraction of phonon transmission and thermal conductance due to longitudinal phonons. Before commenting on the results for the samples with DWs, it is worth observing that the thermal transport is dominated by longitudinal phonons even in the monodomain case (black curves). Nonetheless, the inclusion of a single DW in the channel increases considerably the contribution to the transport from longitudinal phonons, thereby polarizing the thermal flux that crosses the DW. A second and a third DW in a series increase the polarizer effect though they do it in a gradually smaller degree, approaching an asymptotic value in agreement with the results in Fig. 2. The maximal contribution from longitudinal phonons to the conductance (∼75%), and consequently the most polarized thermal flux, is attained at ∼50 K for the sample with three DWs. The polarizer effect is reduced at higher temperatures until it saturates at yet remarkable values. This demonstrates that a series of 180° DWs in PTO works as longitudinal polarizers of high selectivity in lattice thermal transport. We have also explicitly checked that the polarizer effect persists in DWs that are not ideally flat (see Ref. [25] for our tests on this).

The present polarizer effect is clearly originated in the DW scattering of transverse phonons. A finer decomposition of the contribution to the heat transport from transverse modes parallel and perpendicular to the ferroelectric polarization demonstrates that both types are similarly scattered (see Ref. [25]). Thus, bearing in mind the atomic deformations occurring at the 180° DWs, we interpret that, first, the propagation of z-polarized phonons is impeded by the inversion of the ferroelectric distortion across the DWs. Second, since the atomic distortions along the y direction are equivalent, i.e., null, at both sides of the DW, the y-polarized phonons must be scattered by the distortion associated with the occurrence of the P_y polarization at the DW itself (see Fig. 1) [22]. In this regard, we have observed that the parallel or antiparallel orientation of P_y in multiple DW samples does not entail any appreciable difference on the polarizer effect.

Following this reasoning, 180° PTO DWs are transparent for the propagation of longitudinal modes because the components of the atomic distortions along the longitudinal x direction are the same (in particular, null) at both domains and at the DW. Hence, it seems reasonable to predict the opposite effect, i.e., a transverse phonon polarizer, to occur for an alternative configuration of 180° DWs with ferroelectric interfaces perpendicular to the polarization. Such DWs, usually called head-to-head or tail-to-tail, have the peculiarity that the variation of electric displacement across them satisfies Maxwell's relation $\nabla D = \rho_{\text{free}} \neq 0$. As a consequence, these walls can only occur in the presence of free carriers or charged defects, and are difficult to obtain experimentally [29–31]. Yet, our results suggest that they may offer interesting opportunities for filtering effects. (Note that the walls investigated in this work satisfy $\nabla D = 0$. Studying charged DWs would require an explicit treatment of electronic effects in the simulations, and is beyond the scope of the lattice potentials used here.)

In conclusion, we have demonstrated that thermal transport across 180° DWs formed in bulk PTO is sensitive to the polarization of the heat carrying phonons. The propagation of transverse phonons across the DWs is strongly suppressed while, in contrast, the walls are essentially transparent for the longitudinal modes. All in all, 180° DWs behave as longitudinal phonon polarizers of high selectivity whose effect is robust against deviations from the ideal flat shape. Our results also suggest that other DW geometries, such as, e.g., the so-called head-to-head or tail-to-tail configurations, may behave as transverse phonon polarizers. Thereby, multiterminal devices capable of rewriting 180° DWs both parallel and perpendicular to the ferroelectric polarization can be envisaged as dynamically reconfigurable longitudinal/transverse polarizers. Finally, the concept has been here demonstrated for high-frequency heat carrying lattice vibrations due to the narrow width of the ferroelectric walls. Nevertheless, if it were possible to obtain wider DWs, the same principle could apply for longer wavelength phonons, eventually approaching the ultrasound transport regime.

M.R. and R.R. acknowledge financial support by the Ministerio de Economía y Competitividad (MINECO) under Grant No. FEDER-MAT2013-40581-P, by the Severo Ochoa Centres of Excellence Program under Grant No. SEV-2015-0496, by the Generalitat de Catalunya under Grant No.

2014 SGR 301, and through the Beatriu de Pinós fellowship program (2014 BP_B 00101). C.E.S and J.I. are funded by the Luxembourg National Research Fund through the PEARL (Grant No. P12/4853155 COFERMAT), CORE (Grant No. C15/MS/10458889 NEWALLS), and AFR (Ph.D. Grant No. 9934186 for C.E.S.) programs. We thank the Centro de Supercomputación de Galicia (CESGA) for the use of their computational resources.

[1] E. S. Toberer, L. L. Baranowski, and C. Dames, Annu. Rev. Mater. Res. **42**, 179 (2012).
[2] D. G. Cahill, P. V. Braun, G. Chen, D. R. Clarke, S. Fan, K. E. Goodson, P. Keblinski, W. P. King, G. D. Mahan, A. Majumdar, H. J. Maris, S. R. Phillpot, E. Pop, and L. Shi, Appl. Phys. Rev. **1**, 011305 (2014).
[3] M. N. Luckyanova, J. Garg, K. Esfarjani, A. Jandl, M. T. Bulsara, A. J. Schmidt, A. J. Minnich, S. Chen, M. S. Dresselhaus, Z. Ren, E. A. Fitzgerald, and G. Chen, Science **338**, 936 (2012).
[4] J. Ravichandran, A. K. Yadav, R. Cheaito, P. B. Rossen, A. Soukiassian, S. J. Suresha, J. C. Duda, B. M. Foley, C.-H. Lee, Y. Zhu, A. W. Lichtenberger, J. E. Moore, D. A. Muller, D. G. Schlom, P. E. Hopkins, A. Majumdar, R. Ramesh, and M. A. Zurbuchen, Nat. Mater. **13**, 168 (2013).
[5] M. Maldovan, Nat. Mater. **14**, 667 (2015).
[6] G. A. Northrop, E. J. Cotts, A. C. Anderson, and J. P. Wolfe, Phys. Rev. Lett. **49**, 54 (1982).
[7] M. A. Weilert, M. E. Msall, J. P. Wolfe, and A. C. Anderson, Z. Phys. B **91**, 179 (1993).
[8] R. Y. Wang, R. A. Segalman, and A. Majumdar, Appl. Phys. Lett. **89**, 173113 (2006).
[9] C. T. Nelson, P. Gao, J. R. Jokisaari, C. Heikes, C. Adamo, A. Melville, S.-H. Baek, C. M. Folkman, B. Winchester, Y. Gu, Y. Liu, K. Zhang, E. Wang, J. Li, L.-Q. Chen, C.-B. Eom, D. G. Schlom, X. Pan, J. F. Scott, C. A. P. de Araujo *et al.*, Science **334**, 968 (2011).
[10] L. J. McGilly, P. Yudin, L. Feigl, A. K. Tagantsev, and N. Setter, Nat. Nanotechnol. **10**, 145 (2015).
[11] A. V. Ievlev, S. Jesse, A. N. Morozovska, E. Strelcov, E. A. Eliseev, Y. V. Pershin, A. Kumar, V. Y. Shur, and S. V. Kalinin, Nat. Phys. **10**, 59 (2014).
[12] X. Ding and E. K. H. Salje, AIP Adv. **5**, 053604 (2015).
[13] S. Li, X. Ding, J. Ren, X. Moya, J. Li, J. Sun, and E. K. H. Salje, Sci. Rep. **4**, 6375 (2014).
[14] A. Mante and J. Volger, Physica **52**, 577 (1971).
[15] M. A. Weilert, M. E. Msall, A. C. Anderson, and J. P. Wolfe, Phys. Rev. Lett. **71**, 735 (1993).
[16] J. F. Ihlefeld, B. M. Foley, D. A. Scrymgeour, J. R. Michael, B. B. McKenzie, D. L. Medlin, M. Wallace, S. Trolier-McKinstry, and P. E. Hopkins, Nano Lett. **15**, 1791 (2015).
[17] P. E. Hopkins, C. Adamo, L. Ye, B. D. Huey, S. R. Lee, D. G. Schlom, and J. F. Ihlefeld, Appl. Phys. Lett. **102**, 121903 (2013).
[18] J.-J. Wang, Y. Wang, J. F. Ihlefeld, P. E. Hopkins, and L.-Q. Chen, Acta Mater. **111**, 220 (2016).
[19] J. A. Seijas-Bellido, C. Escorihuela-Sayalero, M. Royo, M. P. Ljungberg, J. C. Wojdeł, J. Íñiguez, and R. Rurali, Phys. Rev. B **96**, 140101 (2017).
[20] J. C. Wojdeł, P. Hermet, M. P. Ljungberg, P. Ghosez, and J. Íñiguez, J. Phys.: Condens. Matter **25**, 305401 (2013).
[21] Z. Y. Ong and G. Zhang, Phys. Rev. B **91**, 174302 (2015).
[22] J. C. Wojdeł and J. Íñiguez, Phys. Rev. Lett. **112**, 247603 (2014).
[23] P. Zubko, J. C. Wojdeł, M. Hadjimichael, S. Fernandez-Pena, A. Sené, I. Luk'yanchuk, J.-M. Triscone, and J. Íñiguez, Nature (London) **534**, 524 (2016).
[24] S. Sadasivam, Y. Che, Z. Huang, L. Chen, S. Kumar, and T. S. Fisher, Annu. Rev. Heat Transf. **17**, 89 (2014).
[25] See Supplemental Material at http://link.aps.org/supplemental/10.1103/PhysRevMaterials.1.051402 for a brief description of various technicalities of our calculations and some complementary results and analysis.
[26] A. R. Abramson, C.-L. Tien, and A. Majumdar, J. Heat Transfer **124**, 963 (2002).
[27] W. Zhang, T. S. Fisher, and N. Mingo, J. Heat Transfer **129**, 483 (2007).
[28] Z. Tian, K. Esfarjani, and G. Chen, Phys. Rev. B **89**, 235307 (2014).
[29] M. Y. Gureev, A. K. Tagantsev, and N. Setter, Phys. Rev. B **83**, 184104 (2011).
[30] P. S. Bednyakov, T. Sluka, A. K. Tagantsev, D. Damjanovic, and N. Setter, Sci. Rep. **5**, 15819 (2015).
[31] P. Bednyakov, T. Sluka, A. Tagantsev, D. Damjanovic, and N. Setter, Adv. Mater. **28**, 9498 (2016).